JOURNAL OF Materials CHEMISTRY

A computational study of the effect of doping divalent cations in barite

Fazrie A. Wahid,[a,b] Gillian B. Thomson,[a] Gordon M. Graham[b] and Robert A. Jackson*[c]

[a]*Mechanical and Chemical Engineering Department, Heriot Watt University, Edinburgh, UK EH14 4AS*
[b]*Petroleum Engineering Department, Heriot Watt University, Edinburgh, UK EH14 4AS*
[c]*Lennard-Jones Laboratories, School of Chemistry and Physics, Keele University, Keele, Staffs, UK ST5 5BG. E-mail: r.a.jackson@chem.keele.ac.uk*

Received 20th May 2002, Accepted 5th August 2002
First published as an Advance Article on the web 9th September 2002

The presence of divalent cations during the nucleation of barium sulfate can alter the properties of the nucleated material. Here, a computational study of the effect of doping barium sulfate with divalent cations (Ca^{2+} and Sr^{2+}) is presented. The calculations provide information on the energies and lattice parameter changes involved in the doping process and consequent lattice relaxation. Two methods were used to model the doping process. Firstly, the Mott–Littleton method was used to calculate the solution energy of a single dopant cation in the barite lattice, and secondly, the supercell method was used, which enabled varying dopant concentrations to be modelled. The results were in good agreement with available experimental data.

1 Introduction

The inhibition of sulfate scale is influenced by many factors, including system temperature and pressure,[1] type of scale inhibitor and the qualitative and quantitative ionic content present in the medium.[2,3] Of particular interest in this study is the effect of divalent cations on barium sulfate (barite).

Barium sulfate has been studied in great detail[2–9] due to its presence in water treatment and offshore oil production systems. The abundant presence of divalent cations in the reservoir, for example, during or after the secondary well treatment, could lead to the incorporation of such cations in barium sulfate either during the nucleation phase or the growth phase,[2] or in a complex with an inhibitor which then effectively docks onto the barite surface and promotes inhibition,[10] or in specific cases, reduces inhibitor performance.[11] Experimental evidence has shown that the presence of certain divalent cations can affect the properties of the host barite.[2]

Early attempts at understanding the mechanism of scale inhibition have been carried out by computer modelling[12–14] and experiment.[2–4,15–18] However, no modelling work has yet been carried out on the effect of divalent cations on the bulk barite structure and the subsequent effect on barite inhibition. Early attempts at simulating the role of cations in a barite inhibition system have been carried out,[19] and complex formation involving monovalent cations was proposed.

Recent experimental results have shown that in the presence of calcium ions in a nucleating barium sulfate system, a certain number of calcium ions are actually incorporated into the lattice of barium sulfate; these further promote inhibition efficiency by altering the host lattice properties and theoretically provide a better fit between the inhibitor and the barite surface.[2] In this paper, the results of a computer modelling study on the affinity of divalent cations (Ca^{2+} and Sr^{2+}) to barium sulfate are presented. Two techniques are employed: first, the Mott–Littleton method[20–22] is used to calculate the solution energy for the substitution of an isolated cation in an infinite barite host, and secondly, the supercell method[23] is employed, which enables the energetics of ion substitution and the subsequent lattice deformation to be calculated as a function of ion concentration. All structures were taken from the Inorganic Crystal Structure Database.[24]

2 Computational method

2.1 Interatomic potentials

The potential model employed has been widely used in the modelling of molecular ionic materials.[25,26] It consists of separate terms for non-bonded and bonded interactions. Non-bonded interactions are represented by the Buckingham potential supplemented by an electrostatic term:

$$V_{nb}(r_{ij}) = q_i q_j / r_{ij} + A \exp(-r_{ij}/\rho) - C r_{ij}^{-6}$$

Here, q_i, q_j are the charges on ions i and j (which are not part of the same molecular ion), and A, ρ and C are parameters whose values are obtained for each ion pair by empirical fitting or direct calculation. Charges for the constituent ions in a molecular ion are fitted with the constraint that the ion takes the overall formal charge. Bonded interactions, *i.e.*, in this case, the S–O bond and O–S–O angle of the sulfate group, are represented by harmonic terms:

$$V_b(r, \theta) = 0.5 k_s (r - r_0)^2 + 0.5 k_b (\theta - \theta_0)^2$$

Here, k_s and k_b are bond-stretching and bond-bending force constants, and r_0 and θ_0 are the equilibrium bond length and bond angle, respectively.

For the host lattice and dopant–lattice interactions, the interionic potentials were taken from Allan *et al.*,[27] except that the S–O bonded interaction was refitted as a harmonic potential of the form given above.[26] Potential parameters are given in Table 1.

2.2 Mott–Littleton calculations

The Mott–Littleton method[20–22] is a well-established method for calculating the geometry and energetics of point defects in

Table 1 Potentials and ionic charges used in this study

Buckingham potential			
Interaction	A/eV	ρ/Å	C/eV Å^6
Ba–O	4223.84	0.2907	0.0
Ca–O	1651.35	0.2931	0.0
Sr–O	2509.44	0.2925	0.0
O–O	105 585.02	0.2000	25.98

Harmonic potential		
Interaction	k/eV Å^{-2}	r_0/Å
S–O	150	1.48

Three body potential		
Interaction	k_3/eV rad^{-2}	θ_0/°
O–S–O	15.0	109.47

Ionic charges					
Ion	Ba	Ca	Sr	O	S
Charge/|e|	2.0	2.0	2.0	−0.84	1.36

ionic materials. Briefly, it considers the immediate surroundings of a defect in terms of two concentric spherical regions, with ions within the inner region (region I) being treated explicitly, while a continuum approximation is used for ions in the outer region (region IIB). In this paper, the method is used to model the substitution of a divalent cation at a barium site in an otherwise pure barite system. The energy involved in this process, the defect formation energy, is then converted to a solution energy to enable the substitution of different cations to be compared. Consistent region sizes of 10 (region I) and 15 Å (region IIA) were used throughout this study. The GULP code[28] was used for all calculations.

2.2.1 Solution energy calculations. In order to calculate the energetics of ion substitution, consideration has to be taken of all the steps incorporated in the substitution.[29] In this calculation, it is assumed that the dopant ion is introduced as a sulfate into the barite lattice. The cation, *e.g.* Ca^{2+}, replaces a Ba^{2+} ion, which then combines with the SO_4^{2-} anion to produce a separate barium sulfate phase. The solution energy is the total energy involved in this process, and it gives an indication of the ease of substitution of the dopant ion. An example of calculation of the solution energy for Ca^{2+} in barium sulfate is shown below:

$$CaSO_4 + Ba_{Ba} \rightarrow Ca_{Ba} + BaSO_4$$

The subscript Ba denotes the host cation of interest. The equation above takes into account the source of the dopant ion and any product formed after the substitution has taken place. The solution energy, $E_{solution}$, is calculated as follows, where the lattice energies [*e.g.* $E_{lattice}(CaSO_4)$] are assumed to take negative values, and $E(Ca_{Ba})$ is the defect formation energy for substitution of a Ca^{2+} ion at a Ba^{2+} site.

$$E_{solution} = E(Ca_{Ba}) + E_{lattice}(BaSO_4) - E_{lattice}(CaSO_4)$$

The calculations were then repeated for the other dopant cations. The solution energy was used to give a comparison of relative ease of substitution of the dopant cations in the barite lattice.

2.3 The supercell method

A (2 × 2 × 2) supercell consisting of 192 atoms was generated to simulate the barite host. A single cation substitution was then made in the supercell, and lattice energy minimisation to constant pressure was carried out. The defect energy was obtained from the difference between the lattice energies of the perfect and the defective supercell; the results obtained can be compared to the defect formation energy obtained from the Mott–Littleton method. The calculations could then be repeated with an increasing number of ion substitutions. The doping process involves doping with calcium or strontium ions until all the barium sites were substituted. The calculations enabled the lattice parameter to be calculated as a function of increasing dopant concentration; this was then compared to the predictions of Vegard's law and recent experimental results.[2] Further simulations were later carried out using a (3 × 3 × 3) host supercell to probe lower dopant concentrations.

Table 2 Comparison of ionic and atomic radii of ions involved in this study

	Barium	Calcium	Strontium
Ionic radius/Å	1.34	0.99	1.12
Atomic radius/Å	2.173	1.97	2.15

3 Results and discussion

In this section, the results of the two techniques employed, the Mott–Littleton method and the supercell method, will be used to draw conclusions on barite doping by divalent cations. In Table 2, a comparison of the ionic and atomic radii of the atoms involved in the study is presented. By comparing the ionic radii, it can be seen that strontium has the closest match to a barium ion compared with the calcium ion.

3.1 Results of Mott–Littleton calculations

The defect formation energies for dopant substitution are given in Table 3. Using the technique described in section 2.2.1, the solution energies were then calculated for calcium and strontium dopants in barite (see Table 4); these confirm that strontium substitution would be energetically more favourable than calcium substitution under the conditions of infinite dilution represented by the Mott–Littleton approach. However, due to the nature of the ionic concentration in seawater, particularly in the North Sea, where the concentration of calcium ions is normally higher than strontium ions,[10,11] it can be concluded that, in a real environment, the supersaturation of both ions within the system would play a bigger rôle than their energetics. In any case, the latter do not take into account ion–ion interactions, which are included in the supercell approach described in section 3.2.

3.2 Supercell simulation results

Fig. 1 (representing the data shown in Table 5) shows that the relationship between the unit supercell volume and the amount of dopant follows a linear pattern for strontium and calcium doping. The result for calcium doping is in good agreement with experimental results obtained by Hennessy and Graham, in accordance with the prediction of Vegard's law. Deformation of the host *a*, *b* and *c* axes was calculated at all dopant concentrations.

Fig. 2 illustrates the relationship between the lattice energy and the amount of dopant incorporated in the host lattice for calcium and strontium. The effect of cation doping on lattice

Table 3 Comparison of defect substitution energies

Dopant ion	Defect substitution energy/eV
Ca^{2+}	−1.73
Sr^{2+}	−0.94

Table 4 Comparison of solution energies

Dopant ion	Ca^{2+}	Sr^{2+}
Solution energy/eV	0.49	0.25

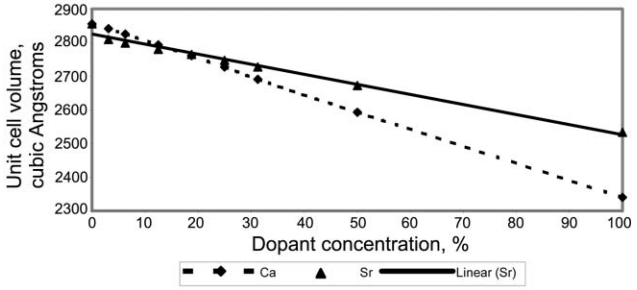

Fig. 1 Plot of unit cell volume *vs.* dopant concentration.

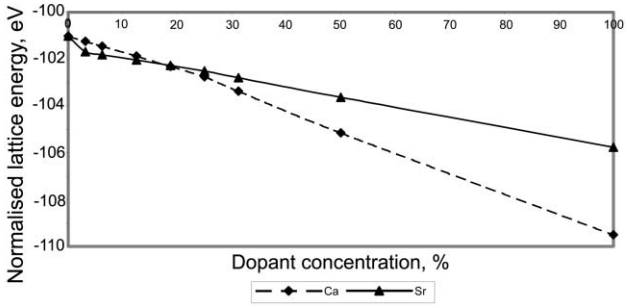

Fig. 2 Normalised lattice energy *vs.* dopant concentration.

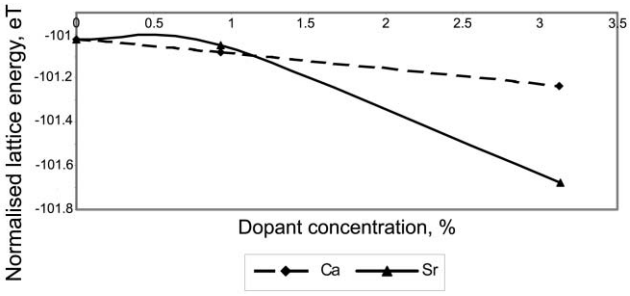

Fig. 3 Normalised lattice energy *vs.* dopant concentration for a 3 × 3 × 3 supercell.

energy was examined and it was found that the introduction of calcium dopants leads to a lower lattice energy after 18% of the available sites in the host are occupied by dopants, while below the 18% level, strontium doping results in the lowest lattice energy. This would imply that strontium dopants are less stable than calcium dopants at dopant levels greater than 18%, but that they are more stable at concentrations below 18%. However, upon performing further calculations using a (3 × 3 × 3) supercell, it was noted that at approximately 0.9% dopant concentration, another transition point occurs (Fig. 3—representing Table 6). Below 0.9% dopant concentration, calcium doping produces the lower lattice energy compared to strontium doping. This implies that between 0.9% and the very low concentrations represented by the Mott–Littleton calculations, calcium doping is more energetically favoured than strontium.

In oilfield conditions, the probability of calcium being incorporated at more than 18% into the lattice of barite is yet to be reported. Hennessy and Graham have reported that the calcium ion has been found to be incorporated into the barium sulfate lattice at up to 12% of the available sites. Furthermore, it can be seen that the substitution of dopants into the lattice would alter its structure. At this level, it is believed that the incorporated calcium would interact with the active inhibitor branch to promote better inhibition,[2] which could be triggered by electrical[30] and mechanical changes[2] in the lattice structure. Further simulations are currently being carried out to study this phenomenon.

It is also possible to calculate the heat of mixing, ΔU, which results from the addition of calcium or strontium to the lattice. This quantity is defined as follows, for calcium substitution:

$$\Delta U = U(\mathrm{CaBaSO_4}) - U(\mathrm{BaSO_4})$$

Here, $U(\mathrm{CaBaSO_4})$ and $U(\mathrm{BaSO_4})$ are the lattice energies of the doped and pure barite lattices, respectively.

Table 5 Lattice energy, heat of mixing and unit cell volume as a function of dopant concentration

% M	No. of M ions	Lattice energy/eV	Normalised lattice energy/eV	Heat of mixing, ΔU/eV	Unit cell volume/Å^3
M = Ca					
0	0	−808.20	−101.03	0.0	2855.67
3.125	1	−809.90	−101.24	−0.21	2841.03
6.25	2	−811.60	−101.45	−0.43	2825.66
12.5	4	−814.94	−101.87	−0.84	2793.01
18.75	6	−818.55	−102.32	−1.29	2760.82
25	8	−822.04	−102.76	−1.73	2727.42
31.25	10	−826.94	−103.37	−2.34	2691.24
50	16	−841.20	−105.15	−4.12	2592.88
100	32	−876.03	−109.50	−8.47	2339.83
M = Sr					
0	0	−808.20	−101.03	0.0	2855.67
3.125	1	−813.44	−101.68	−0.65	2809.32
6.25	2	−814.50	−101.81	−0.78	2798.63
12.5	4	−816.35	−102.04	−1.01	2780.23
18.75	6	−818.18	−102.27	−1.24	2764.51
25	8	−820.07	−102.51	−1.48	2747.13
31.25	10	−822.33	−102.79	−1.76	2727.31
50	16	−829.06	−103.63	−2.60	2671.86
100	32	−846.07	−105.76	−4.73	2533.02

Table 6 Comparison of lattice energy and heat of mixing at very low dopant concentration

Dopant ion	Amount	%	Lattice energy/eV	Normalised lattice energy/eV	Heat of mixing, ΔU/eV
Sr	1	0.93	−2728.37	−101.05	−0.02
Ca	1	0.93	−2729.06	−101.08	−0.05

By comparing the elastic constants from the doping process, it was possible to monitor the elasticity changes in the structure. Changes in the structural parameters could also be monitored. For example, when barite is progressively doped with strontium, barytocelestine ($Ba_{0.5}Sr_{0.5}SO_4$) is initially formed, and then, after 100% substitution, celestine ($SrSO_4$) is formed, with good reproduction of the lattice parameters. This is in good agreement with the work of Grahmann, reported by Deer *et al.*[31]

4 Conclusions

The Mott–Littleton calculations have shown that under conditions of infinite dilution, strontium substitution would be favoured over calcium substitution in barite. The supercell calculations have shown that the relative affinity of the two ions depends on their concentration, with calcium substitution being favoured at concentrations below 0.9% and over 18%. Finally, the calculations reproduce the experimentally observed lattice contraction of barite as calcium concentration is increased.

The calculations presented in this paper have concentrated on the substitution of dopants into the bulk crystal; future calculations will consider the substitution of dopants at crystal surfaces and their effect on morphology, following an approach recently applied to cobalt doping of calcite.[32]

Acknowledgements

The authors acknowledge use of the EPSRC Chemical Database Service at Daresbury, and wish to thank Dr Julian Gale for the GULP code used in this study, and Dr Alison Hennessy for fruitful discussions and help. F. A. W. and G. M. G. thank their group sponsors for financial support.

References

1 G. M. Graham, M. M. Jordan, G. C. Graham, W. Sablerolle, K. S. Sorbie, P. Hill and J. Bunney, *SPE J.*, 1997, 37 274.
2 A. J. B. Hennessy and G. Graham, *J. Cryst. Growth*, 2002, **237**, 2153.
3 S. N. Black, L. A. Bromley, D. Cottier, R. J. Davey, B. Dobbs and J. E. Rout, *J. Chem. Soc., Faraday Trans.*, 1991, **87**(20), 3409.
4 H. Espig and H. Neels, *Krist. Tech.*, 1967, **2**, 401.
5 B. R. Heywood and S. Mann, *J. Am. Chem. Soc.*, 1992, **114**, 4681.
6 R. J. Davey, S. N. Black, L. A. Bromley, D. Cottier and J. E. Rout, *Nature*, 1991, **353**, 549.
7 P. Dawson, M. M. Hargreave and G. R. Wilkinson, *Spectrochim. Acta, Part A*, 1977, **33**, 83.
8 W. J. Benton, I. R. Collins, I. M. Grimsey, G. M. Parkinson and S. A. Rodger, *Faraday Discuss.*, 1993, **95**, 281.
9 R. T. Barthorpe, *Corrosion 92, The NACE Annual Conference and Corrosion Show*, National Association of Corrosion Engineers, Houston, 1992, paper no. 2.
10 G. M. Graham, L. S. Boak and K. S. Sorbie, *SPE J.*, 1997, 37 273.
11 L. S. Boak, G. M. Graham and K. S. Sorbie, *SPE J.*, 1999, 50 771.
12 S. Gill and R. G. Varsanik, *J. Cryst. Growth*, 1986, **76**, 57.
13 A. L. Rohl, D. H. Gay, R. J. Davey and C. R. A. Catlow, *J. Am. Chem. Soc.*, 1996, **118**, 642.
14 C. R. A. Catlow, J. D. Gale, D. H. Gay, M. A. Nygren and D. C. Sayle, *Interfacial Science*, Chemistry for the 21st Century, Monograph no. 195, International Union of Pure and Applied Chemistry, Research Triangle Park, NC, 1997.
15 M. C. van der Leeden and G. M. Rosmalen, *SPE J.*, 1998, 17 914.
16 M. C. van der Leeden, J. Reedijk and M. van Rosmalen, *Estud. Geol.*, 1982, 279.
17 W. H. Leung and G. H. Nancollas, *J. Cryst. Growth*, 1978, **44**, 163.
18 Z. Berkovitchyellin, J. Van Mil, L. Addadi, M. Idelson, M. Lahav and L. Leiserowitz, *J. Am. Chem. Soc.*, 1985, **107**, 3111.
19 M. Blanco, Y. Tang, P. Shuler and W. Goddard, *Mol. Eng.*, 1997, **7**, 491.
20 N. F. Mott and M. J. Littleton, *Trans. Faraday Soc.*, 1938, **34**, 485.
21 A. B. Lidiard, *J. Chem. Soc., Faraday Trans. 2*, 1989, **85**(5), 341.
22 C. R. A. Catlow, *J. Chem. Soc., Faraday Trans. 2*, 1989, **85**(5), 335.
23 R. A. Jackson, J. E. Huntington and R. G. J. Ball, *J. Mater. Chem.*, 1991, **1**(6), 1079.
24 D. A. Fletcher, R. F. McMeeking and D. Parkin, *J. Chem. Inf. Comput. Sci.*, 1996, **36**, 746.
25 R. A. Jackson, G. D. Price, P. Meenan, K. J. Roberts, G. B. Telfer and P. J. Wilde, *Mineral. Mag.*, 1995, **59**, 617.
26 R. A. Jackson, *Curr. Opin. Solid State Mater. Sci.*, 2001, **5**, 463.
27 N. L. Allan, A. L. Rohl, D. H. Gay, C. R. A. Catlow, R. J. Davey and W. C. Mackrodt, *Faraday Discuss.*, 1993, **95**, 273.
28 J. D. Gale, *J. Chem. Soc., Faraday Trans.*, 1997, **93**(4), 629.
29 R. A. Jackson, M. E. G. Valerio and J. F. de Lima, *J. Phys. Condens. Matter*, 2001, **13**, 2147.
30 I. R. Collins, *J. Colloid Interface Sci.*, 1999, **212**, 535.
31 W. A. Deer, R. A. Howie and J. Zussman, *An Introduction to the Rock Forming Minerals*, Longman, London, 2nd edn., 1992.
32 A. L. Braybrook, B. R. Heywood, R. A. Jackson and K. Pitt, *J. Cryst. Growth*, 2002, **243**, 336.